ALBERT-LUDWIGS-UNIVERSITÄT FREIBURG
INSTITUT FÜR INFORMATIK

Lehrstuhl für Mustererkennung und Bildverarbeitung

Fourier Analysis in Polar and Spherical Coordinates

Internal Report 1/08

Qing Wang, Olaf Ronneberger, Hans Burkhardt

Fourier Analysis in Polar and Spherical Coordinates

Qing Wang, Olaf Ronneberger, Hans Burkhardt

Abstract

In this paper, polar and spherical Fourier Analysis are defined as the decomposition of a function in terms of eigenfunctions of the Laplacian with the eigenfunctions being separable in the corresponding coordinates. Each eigenfunction represents a basic pattern with the wavenumber indicating the scale. The proposed transforms provide an effective radial decomposition in addition to the well-known angular decomposition. The derivation of the basis functions is compactly presented with an emphasis on the analogy to the normal Fourier transform. The relation between the polar or spherical Fourier transform and normal Fourier transform is explored. Possible applications of the proposed transforms are discussed.

1 Introduction

Fourier transform is very important in image processing and pattern recognition both as a theory and as a tool. Usually it is formulated in Cartesian coordinates, where a separable basis function in 3D space without normalization is

$$e^{i\mathbf{k}\cdot\mathbf{r}} = e^{ik_x x} e^{ik_y y} e^{ik_z z} \tag{1}$$

where (x, y, z) are coordinates of the position $\mathbf{r}$ and k_x, k_y, k_z are components of the wave vector $\mathbf{k}$ along the corresponding axis. The basis function (1) represents a plane wave. Fourier analysis is therefore the decomposition of a function into plane waves. As the basis function is separable in x, y and z, The decomposition can be understood as being made up of three decompositions (for 3D).

The Laplacian is an important operator in mathematics and physics. Its eigenvalue problem gives the time-independent wave equation. In Cartesian coordinates the operator is written as

$$\boldsymbol{\nabla}^2 = \nabla_x^2 + \nabla_y^2 + \nabla_z^2 = \frac{\partial^2}{\partial x^2} + \frac{\partial^2}{\partial y^2} + \frac{\partial^2}{\partial z^2} \ .$$

for 3D space. (1) is an eigenfunction of the Laplacian and is separable in Cartesian coordinates.

When defined on the whole space, functions given in (1) are mutually orthogonal for different $\mathbf{k}$; wave vectors take continuous values and it is said that one has a continuous spectrum. Over finite regions, the mutual orthogonality generally does not hold. To get an orthogonal basis, $\mathbf{k}$ can only take values from

a discrete set and the spectrum becomes discrete. The continuous Fourier transform reduced to Fourier series expansion (with continuous spatial coordinates) or to the discrete Fourier transform (with discrete spatial coordinates).

For objects with certain rotational symmetry, it is more effective for them to be investigated in polar (2D) or spherical (3D) coordinates. It would be of great advantage if the image can be decomposed into wave-like basic patterns that have simple radial and angular structures, so that the decomposition is made up of radial and angular decompositions. Ideally this decomposition should be an extension of the normal Fourier analysis and can therefore be called Fourier analysis in the corresponding coordinates. To fulfill these requirements, the basis functions should take the separation-of-variable form:

$$R(r)\Phi(\varphi) \tag{2}$$

for 2D and

$$R(r)\Theta(\vartheta)\Phi(\varphi) = R(r)\,\Omega(\vartheta,\varphi) \tag{3}$$

for 3D where (r,φ) and (r,ϑ,φ) are the polar and spherical coordinates respectively. They should also be the eigenfunctions of the Laplacian so that they represent wave-like patterns and that the associated transform is closely related to the normal Fourier transform. The concrete form of the angular and radial parts of the basis functions will be investigated and elaborated in the coming sections but will be briefly introduced below in order to show previous work related to them.

For polar coordinates, as will be shown in the next section, the angular part of a basis function is simply

$$\Phi(\varphi) = \frac{1}{\sqrt{2\pi}} e^{im\varphi} \tag{4}$$

where m is an integer, which is a natural result of the single-value requirement: $\Phi(\varphi) = \Phi(\varphi + 2\pi)$, a special kind of boundary condition. The associated transform in angular coordinate is nothing else but the normal 1D Fourier transform. For spherical coordinates, the angular part of a basis function is a spherical harmonic

$$\Omega(\vartheta,\varphi) = Y_{lm}(\vartheta,\varphi) = \sqrt{\frac{2l+1}{4\pi}\frac{(l-m)!}{(l+m)!}} P_{lm}(\cos\vartheta) e^{im\varphi} \tag{5}$$

where P_{lm} is an associated Legendre polynomial and l and m are integers, $l \geq 0$ and $|m| \leq l$. It also satisfies the single-value requirement. The corresponding transform is called Spherical Harmonic (SH) transform and has been widely used in representation and registration of 3D shapes [8–10].

The angular parts of the transforms in 2D and 3D are therefore very familiar. Not so well-known are the transforms in the radial direction. The radial basis function is a Bessel function $J_m(kr)$ for polar coordinates and a spherical Bessel function $j_l(kr)$ for spherical coordinates. In both cases, The parameter k can take either continuous or discrete values, depending on whether the region is infinite or finite. For functions defined on $(0,\infty)$, the transform with $J_m(kr)$ as integral kernel and r as weight is known as the Hankel transform. For functions

defined on a finite interval, with zero-value boundary condition for the basis functions, one gets the Fourier-Bessel series [1]. Although the theory on Fourier-Bessel series has long been available, it mainly has applications in physics-related areas [18, 19]. [12] and a few references therein are the only we can find that employ Fourier-Bessel series expansion for 2D image analysis. Methods based on Zernike moments are on the other hand much more popular in applications where we believe the Fourier-Bessel expansion also fits. The Zernike polynomials are a set of orthogonal polynomials defined on a unit disk, which have the same angular part as (4).

The SH transform works on the spherical surface. When it is used for 3D volume data, the SH features (extracted from SH coefficients) can be calculated on concentric spherical surfaces of different radii and be collected to describe an object, as suggested in [9]. This approach treats each spherical surface as independent to one another and has a good localization nature. it fails to describe the relation of angular properties of different radius as a whole, therefore cannot represent the radial structures effectively. The consideration of how to describe the radial variation of the SH coefficients actually motivated the whole work presented here.

In this paper, the operations that transform a function into the coefficients of the basis functions given in (2) and (3) and described above will simply be called *polar* and *spherical Fourier transform* respectively. It should be noted though that in the literature, the former often refers to the normal Fourier transform with wave vectors $\mathbf{k}$ expressed in polar coordinates (k, φ_k) [16] and the latter often refers to the SH transform [17].

Due to the extreme importance of the Laplacian in physics, the expansion of functions with respect to its eigenfunctions is naturally not new there. For example, in [20] and [21], the eigenfunctions of the Laplacian are used for expansion of sought wave functions. The idea that these eigenfunctions can be used as basis functions for analyzing 2D or 3D images is unfamiliar to the pattern recognition society. There also lacks a simple and systematic presentation of the expansion from the point of view of signal analysis. Therefore, although parts of the derivation are scattered in books like [1], we rederive the basis functions to emphasize the analogy to the normal Fourier transform. Employment of the Sturm-Liouville theory makes this analogy clearer and the derivation more compact.

The proposed polar and spherical Fourier transforms are connected with the normal Fourier transform by the Laplacian. We investigate the relations between them so that one can understand the proposed transforms more completely and deeply. It is found that the relations also provide computational convenience. An advantage of the proposed transforms is that when a function is rotated around the origin, the change of its transform coefficients can be relatively simply expressed in terms of the rotation parameters. This property can, on the one hand, be used to estimate rotation parameters, on the other hand, be used to extract rotation-invariant descriptors. We will show how to do them.

Section 2 deals with the polar Fourier transform. Besides presentation of the theory, issues about calculation of the coefficients are discussed. A short comparison between polar Fourier basis functions and Zernike functions is made at the end. Parallel to section 2, the theory for the spherical Fourier transform is given in section 3. In section 4 we investigate the possible applications of the

polar and spherical Fourier transforms. At the end, conclusion and outlook are given.

2 Polar Fourier transform

2.1 Basis Functions

2.1.1 Helmholtz Equation and Angular Basis Functions

As a direct extension from the Cartesian case, we begin with the eigenfunctions of the Laplacian, whose expression in polar coordinates is given by:

$$\boldsymbol{\nabla}^2 = \nabla_r^2 + \frac{1}{r^2}\nabla_\varphi^2 \tag{6}$$

where

$$\nabla_r^2 = \frac{1}{r}\frac{\partial}{\partial r}\left(r\frac{\partial}{\partial r}\right) \tag{7}$$

and

$$\nabla_\varphi^2 = \frac{\partial^2}{\partial \varphi^2} \ . \tag{8}$$

are the radial and angular parts. The eigenvalue problem can be written as

$$\nabla_r^2\Psi(r,\varphi) + \frac{1}{r^2}\nabla_\varphi^2\Psi(r,\varphi) + k^2\Psi(r,\varphi) = 0 \ , \tag{9}$$

which is the Helmholtz differential equation in polar coordinates. We require that $k^2 \geq 0$ as with negative k^2, the radial functions are exponentially growing or decaying, which are not interesting for our purpose. It will be shown later that such a requirement does not prevent the eigenfunctions from forming a basis. For simplicity, it is further required that $k \geq 0$. Substituting the separation-of-variable form $\Psi(r,\varphi) = R(r)\Phi(\varphi)$ into (9), one gets

$$\frac{\partial^2}{\partial \varphi^2}\Phi + m^2\Phi = 0 \tag{10}$$

$$\frac{1}{r}\frac{\partial}{\partial r}\left(r\frac{\partial}{\partial r}\right)R + \left(k^2 - \frac{m^2}{r^2}\right)R = 0 \ . \tag{11}$$

The solution to (10) is simply

$$\Phi_m(\varphi) = \frac{1}{\sqrt{2\pi}}e^{im\varphi} \tag{12}$$

with m being an integer.

2.1.2 Radial Basis Functions

The general solution to (11) is

$$R(r) = AJ_m(kr) + BY_m(kr) \tag{13}$$

where J_m and Y_m are the m-th order Bessel functions and Neumann functions respectively [1]; A and B are constant multipliers. A nonsingular requirement of R at the origin leaves

$$R(r) = J_m(kr) \tag{14}$$

as Y_m is singular at the origin. Bessel functions satisfy the orthogonality relation

$$\int_0^\infty J_m(k_1 r) J_m(k_2 r) r dr = \frac{1}{k_1}\delta(k_1 - k_2) \tag{15}$$

just like the complex exponential functions satisfy

$$\int_{-\infty}^{\infty} e^{ik_1 x} \left[e^{ik_2 x}\right]^* dx = 2\pi\, \delta(k_1 - k_2) \ . \tag{16}$$

Actually $J_m(kr)$ forms a basis for functions defined on $(0, \infty)$ and satisfied certain continuous and integrable conditions (Later this kind of description is understood when we talk about functions to be transformed or to be expanded).

For the Fourier transform, an infinite space corresponds to a continuous spectrum and a finite space corresponds to a discrete spectrum, where proper boundary conditions select the spectrum. The same is also true for the radial basis functions in polar coordinates. Over the finite interval $[0, a]$, the orthogonal relation like in (15) generally does not hold any more, instead,

$$\begin{aligned} & \int_0^a J_m(k_1 r) J_m(k_2 r) r dr \\ = \ & \frac{a}{k_1^2 - k_2^2}\left[k_2 J_m(k_1 a) J_m'(k_2 a) - k_1 J_m(k_2 a) J_m'(k_1 a)\right]. \end{aligned} \tag{17}$$

By imposing boundary conditions according to the Sturm-Liouville (S-L) theory [2, 5], a set of k values can be determined that make $J_m(kr)$ again mutually orthogonal. We first rewrite (11) as

$$-(rR')' + \frac{m^2}{r}R = k^2 rR. \tag{18}$$

With

$$\begin{cases} p(r) = r \\ q(r) = \frac{m^2}{r} \\ w(r) = r \\ \lambda = k^2 \end{cases} , \tag{19}$$

the equation (18) takes the S-L form:

$$-\left(p(r)R'\right)' + q(r)R = \lambda w(r) R \tag{20}$$

where $r \in [0, a]$. Eq.(20) together with the following boundary conditions forms a S-L system.

$$\begin{cases} R(0)\cos\alpha - p(0)R'(0)\sin\alpha = 0 \\ R(a)\cos\beta - p(a)R'(a)\sin\beta = 0 \end{cases} \tag{21}$$

where $\alpha, \beta \in [0, \pi)$. The allowed values of λ are called the eigenvalues of the system. According to the theory, for such a S-L system,

1. The eigenvalues are nonnegative real numbers and can be numbered to form an increasing sequence $\lambda_1 < \lambda_2 < \cdots < \lambda_n < \cdots$;

2. The corresponding eigenfunctions can be uniquely determined up to a costant multiplier;

3. The eigenfunctions are mutually orthogonal with respect to the weight function $w(r) = r$;

4. The n-th eigenfunction has exactly $n - 1$ zeros on the interval $(0, a)$;

5. The complete set of eigenfunctions forms a complete orthogonal set of functions defined on the interval $[0, a]$.

Since $R(r) = J_m(kr)$ is a general non-singular solution to (20), the values k can take (therefore the eigenvalues $\lambda = k^2$) are determined by the boundary conditions (21). With $\alpha = \pi/2$, the first equation in (21) has actually no effect on the selection of k but Y_m can be excluded from the general solution (13) if we have not done so. The only effective boundary condition left is the second equation in (21). Substituting $R(r) = J_m(kr)$ into it, one gets

$$J_m(ka)\cos\beta - kaJ'_m(ka)\sin\beta = 0 \tag{22}$$

with $x = ka$, (22) becomes

$$J_m(x)\cos\beta - xJ'_m(x)\sin\beta = 0 \tag{23}$$

Suppose $(x_{m1} < x_{m2} < \cdots < x_{mn} < \cdots)$ are nonnegative solutions to (23) with $J_m(x_{mn}r/a)$ being nonzero functions, then k can take the values from

$$\left\{ \frac{x_{m1}}{a}, \frac{x_{m2}}{a}, \cdots, \frac{x_{mn}}{a}, \cdots \right\} \ .$$

Define

$$k_{nm} = \frac{x_{mn}}{a} \tag{24}$$

(The indices n and m now exchange their order for the sake of convention), the n-th eigenvalue is then $\lambda_n = k_{nm}^2$ and the n-th eigenfunction is $J_m(k_{nm}r)$. The orthogonality of the eigenfunctions can be written as

$$\int_0^a J_m(k_{nm}r)J_m(k_{n'm}r)rdr = N_n^{(m)}\delta_{nn'} \ . \tag{25}$$

By taking the limit of (17) as $k_2 \to k_1$ and taking into account that $J_m(kr)$ is the solution to (11), one can get

$$N_n^{(m)} = \frac{a^2}{2}\left[{J'_m}^2(x_{mn}) + \left(1 - \frac{m^2}{x_{mn}^2}\right) J_m^2(x_{mn}) \right] \ . \tag{26}$$

The normalized radial function can therefore be defined as

$$R_{nm}(r) = \frac{1}{\sqrt{N_n^{(m)}}} J_m(k_{nm}r) \ . \tag{27}$$

$\{R_{nm}|n = 1, 2, \cdots\}$ forms an orthonormal basis on the interval $[0, a]$. A function $f(r)$ defined on this interval can be expanded as

$$f(r) = \sum_{n=1}^{\infty} \left[\int_0^a f(\rho) R_{nm}(\rho) \rho d\rho \right] R_{nm}(r) \ . \tag{28}$$

So far β in (23) has not been specified. Two cases are interesting:
Zero-value boundary condition: with $\sin\beta = 0$, (23) reduces to

$$J_m(x) = 0 \ . \tag{29}$$

(note that $x = ka$). x_{mn} should be the positive zeros of $J_m(x)$. Under this condition,

$$N_n^{(m)} = \frac{a^2}{2} J_{m+1}^2(x_{mn}) \tag{30}$$

and the right-hand side of (28) is usually known as m-th order Fourier-Bessel series of $f(r)$.
Derivative boundary condition: with $\cos\beta = 0$, (23) becomes

$$J'_m(x) = 0 \ . \tag{31}$$

x_{mn} should be the zeros of $J'_m(x)$. One special case needs to be considered here: $x = 0$ is one solution to $J'_0(x) = 0$ and $J_0(0 \cdot r/a) = 1$ has exactly 0 zero on $(0, a)$. According to the S-L theory, $x = 0$ should be recognized as x_{01}. Under this boundary condition,

$$N_n^{(m)} = \frac{a^2}{2} \left(1 - \frac{m^2}{x_{mn}^2} \right) J_m^2(x_{mn}) \tag{32}$$

with the special case $N_1^{(0)} = a^2/2$.

It is clear now that different boundary conditions lead to different spectra of the system. The choice should depend on the problems under investigation. To give an impression how the radial functions look like, we show the first few of them for $m = 2$ with the zero and the derivative boundary conditions in Fig. 1 (a) and (b). It is intuitive to choose the zero boundary condition when the images tend to be zero at $r = a$ and the derivative condition when the image tend to be constant in radial direction near $r = a$. Often it is necessary to do some experiments to find the better choice.

$R_{nm}(r)$ has $n - 1$ zeros on $(0, a)$. Its wave-like property can be made more clear by considering the asymptotic behavior of the Bessel functions [1]. One has

$$R_{nm}(r) \sim \frac{1}{\sqrt{r}} \cos\left(k_{nm} r - \frac{m\pi}{2} - \frac{\pi}{4} \right) \tag{33}$$

for $k_{nm} r \gg |m^2 - \frac{1}{4}|$. Therefore, with large $k_{nm} r$, $R_{nm}(r)$ approaches a cosine function with its amplitude decreasing as fast as $1/\sqrt{r}$. There is a phase shift of $-(m\pi/2 + \pi/4)$, which is corresponded to by a "delay" of the function to take the wave-like form near the origin. See Fig. 6 (a) for a typical form of $R_{nm}(r)$ with relatively large n and m.

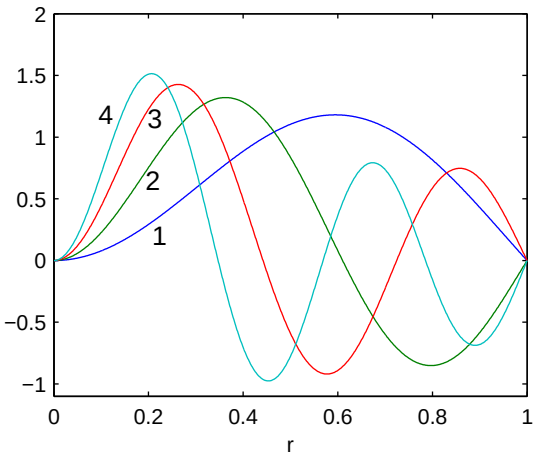

(a)

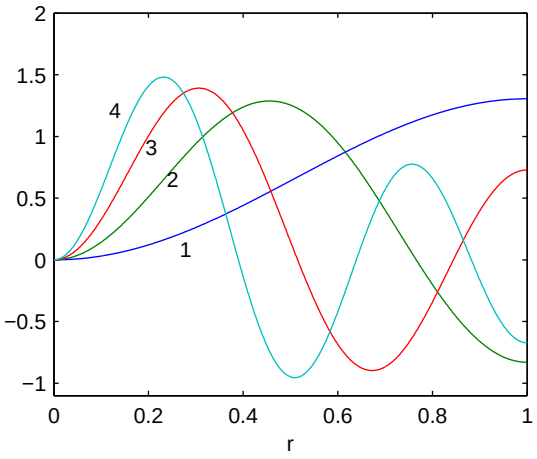

(b)

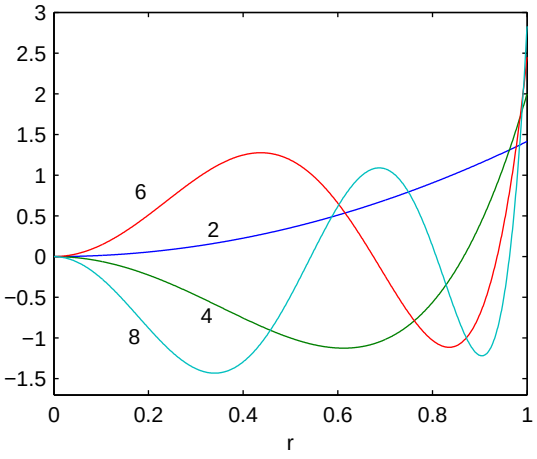

(c)

Figure 1: The first few radial basis functions for 2D with $m = 2$ and $a = 1$: (a) R_{nm} with zero boundary condition; (b) R_{nm} with derivative boundary condition and (c) normalized radial Zernike function $\widetilde{Z}_{nm}$. The number beside each curve is the value of n.

2.1.3 Basis Functions

The basis function for the polar Fourier transform is composed of the radial and the angular parts. Consequently, for the transform defined on the whole space, the basis function is given by

$$\Psi_{k,m}(r,\varphi) = \sqrt{k} J_m(kr)\Phi_m(\varphi) \tag{34}$$

with k taking continuous nonnegative values and Φ_m defined by (12). For the transform defined on the finite region $r \le a$, the basis function is given by

$$\Psi_{nm}(r,\varphi) = R_{nm}(r)\Phi_m(\varphi) \tag{35}$$

with R_{nm} defined by (27). The orthogonality relation is given by:

$$\int_0^a \int_0^{2\pi} \Psi^*_{nm}(r,\varphi)\Psi_{n'm'}(r,\varphi) r dr d\varphi = \delta_{nn'}\delta_{mm'} \ . \tag{36}$$

A basis function satisfies the following equation as well as the corresponding boundary conditions

$$\nabla^2 \Psi_{nm} + k^2_{nm}\Psi_{nm} = 0 \ . \tag{37}$$

$\{\Psi_{nm}\}$ with $(n = 1, 2, \cdots)$ and $(m = \cdots, -2, -1, 0, 1, 2, \cdots)$ form an orthonormal basis on the region $r \le a$.

For $\Psi_{nm}(r,\varphi)$, m is the number of periods in the angular direction, and $n-1$ corresponds to the number of zero crossings in the radial direction. As for the meaning of k_{nm}, those who are familiar with quantum mechanics can recognize from (37) that k^2_{nm} is the energy level (except for a constant factor) of the system and its corresponding wave function is Ψ_{nm}. Some of the functions with lowest energy levels are shown in Figure 2. One can find that the higher the energy level, the finer the structures. Therefore for image analysis, the value of k is an indication of the scale of the basic patterns, which is consistent with the normal Fourier transform.

2.2 Expansion

A 2D function $f(r,\varphi)$ defined on the whole space can be expanded with respect to $\Psi_{k,m}$ as defined in (34):

$$f(r,\varphi) = \int_0^\infty \sum_{m=-\infty}^{\infty} P_{k,m}\Psi_{k,m}(r,\varphi)\, k dk \tag{38}$$

where

$$P_{k,m} = \int_0^\infty \int_0^{2\pi} f(r,\varphi)\Psi^*_{k,m}(r,\varphi) r dr d\varphi \tag{39}$$

are the polar Fourier coefficients (P stands for Polar). The infinite transform as given in (38) and (39) is mainly of theoretical interest. In practice, one should use the transform defined on a finite region. A function $f(r,\varphi)$ defined on $r \le a$ can be expanded with respect to $\{\Psi_{nm}\}$ (It is understood with this symbol that n and m are integers and n is positive) as

$$f(r,\varphi) = \sum_{n=1}^{\infty} \sum_{m=-\infty}^{\infty} P_{nm}\Psi_{nm}(r,\varphi) \tag{40}$$

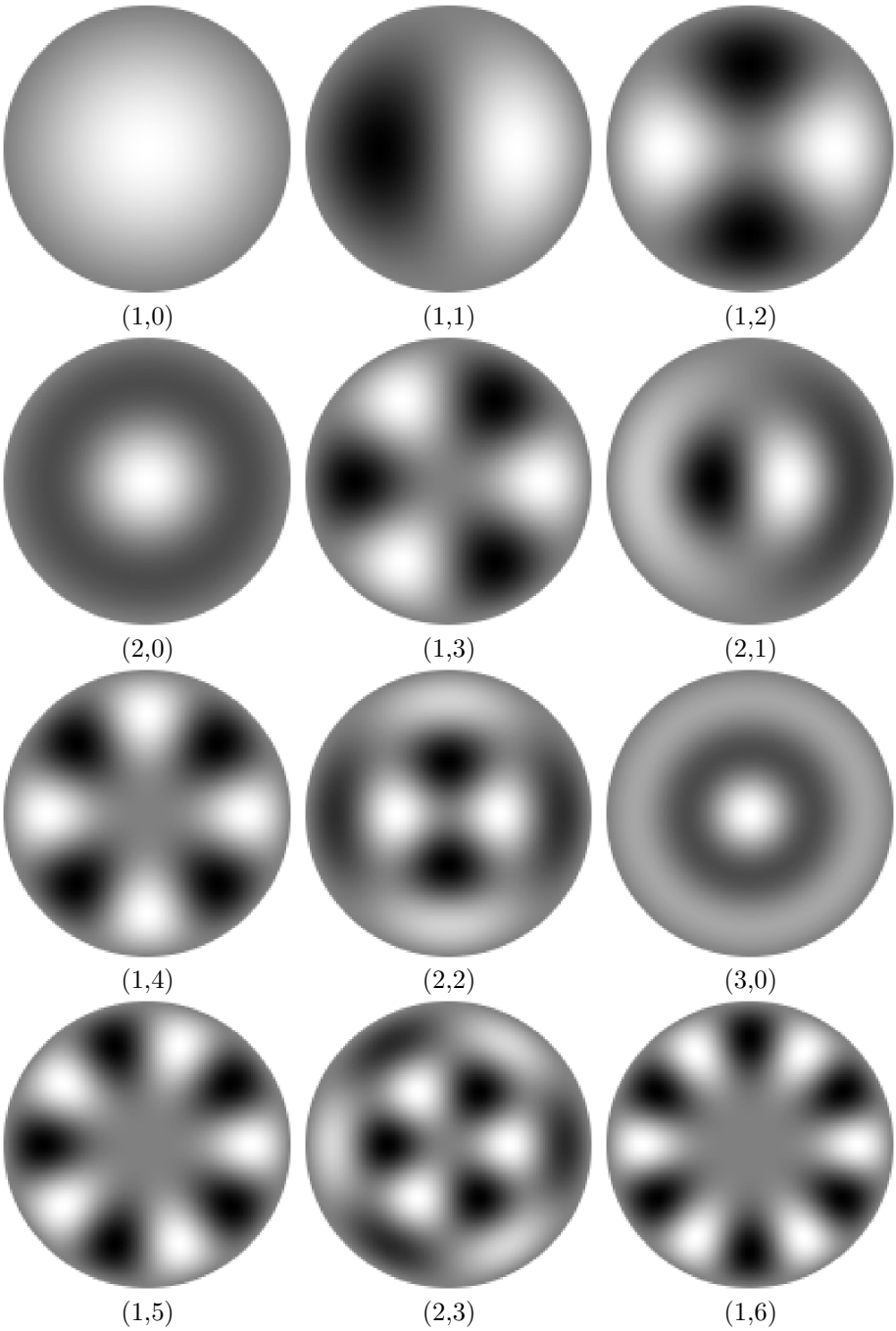

Figure 2: Basic patterns represented by Ψ_{nm} with zero boundary condition. Shown are the real part of the functions. (n, m) pairs are given under each pattern. The patterns are listed in the increasing order of the value of k_{nm}.

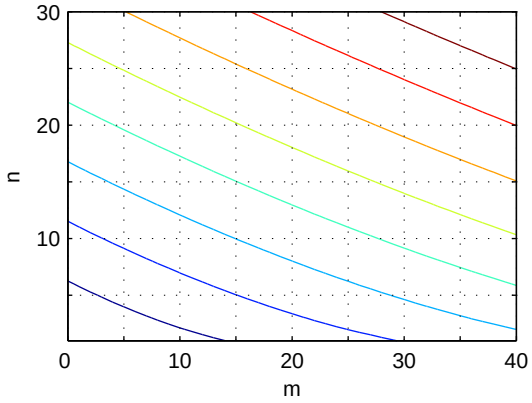

Figure 3: Isolines of k_{nm}

where the coefficients

$$P_{nm} = \int_0^a \int_0^{2\pi} f(r,\varphi)\Psi_{nm}^*(r,\varphi) r dr d\varphi \ . \tag{41}$$

There are two indices for the expansion. How should the terms be ordered and therefore be truncated for a finite-term expansion? A natural way is according to the energy levels. In the language of image analysis, according to the scales of the basic patterns. Larger-scale patterns should be taken into account first. This is often the best choice if no other information about the data is available. Figure 3 shows the isolines of k_{nm}.

A digital image is usually given on an equally-spaced grid in Cartesian coordinates. To evaluate the coefficients as in (41), it is advisable to map the image I into polar coordinates, where the transform becomes separable and the angular part can be done fast with FFT. The grid density of the mapped image I_{polar} should be high enough to accommodate the finest patterns in the expansion. Let the largest values for m and k_{nm} be $m_{\max}$ and $k_{\max}$. Denote the radial and angular size of I_{polar} as M_r and M_φ. The sampling theorem requires

$$M_\varphi \geq 2m_{\max} \ . \tag{42}$$

M_φ should also be chosen to facilitate fast calculations.

Considering the asymptotic behavior of $R_{nm}(r)$ in (33), k_{nm} takes the position of the wavenumber. One can expect that M_r should be at least

$$2 \cdot \frac{a}{2\pi/k_{\max}} = \frac{ak_{\max}}{\pi} \ .$$

However, the right-hand side of (33) is only the asymptotic bahavior and is not a real trigonometric function. Furthermore, the weight function is r instead of 1 for the radial integral. It is necessary to do some numerical experiments to determine the number of sampling points M_r in order to ensure that (25) holds within a certain relative error.

Mapping of the image is a process of interpolating and sampling. It must be handled carefully to avoid aliasing. The finest structure supported in both

radial and angular directions should match the finest structure in Cartesian coordinates. Approximately, that means, for a disk of radius a (in the unit of a pixel) in the original image, there should be $\sqrt{2}a$ steps in r and $2\sqrt{2}\pi a$ steps in φ. The $\sqrt{2}$ inside the expressions comes from the fact than the highest frequency for the original image is $\sqrt{2}/2$ instead of $1/2$. Often $\sqrt{2}$ can be dropped if one is sure that there is no so fine structure in the original image, which is usually obeyed for image taking. If M_r and M_φ are smaller than these numbers, in other words, the resolution in I_{polar} is coarser than in the original image I, one can either first smooth I then perform the mapping, or alternatively, first map I to polar coordinates with proper resolutions followed by smoothing and downscaling in r or φ. Which approach to take depends on the aspect ratio of I_{polar}.

2.3 Relation to the Normal Fourier Transform in 2D

2.3.1 Infinite Transform

To find the relation between the polar and the normal Fourier transforms, one needs to know the relation of their bases. The basis function for normal Fourier transform represents a plane wave:

$$\frac{1}{2\pi}e^{i\mathbf{k}\cdot\mathbf{r}} = \frac{1}{2\pi}e^{ikr\cos(\varphi-\varphi_k)} \quad . \tag{43}$$

where $\mathbf{k}$ is the wave vector and (k, φ_k) and (r, φ) are the polar coordinates of $\mathbf{k}$ and $\mathbf{r}$ respectively. The basis function is defined on the whole space and can be expanded according to the Jacobi-Anger Identity [6] as

$$\begin{aligned}
\frac{1}{2\pi}e^{i\mathbf{k}\cdot\mathbf{r}} &= \frac{1}{2\pi}e^{ikr\cos(\varphi-\varphi_k)} \\
&= \sum_{m=-\infty}^{\infty} i^m \frac{1}{2\pi} J_m(kr) e^{im(\varphi-\varphi_k)} \\
&= \sum_{m=-\infty}^{\infty} \frac{i^m}{\sqrt{2\pi k}} e^{-im\varphi_k} \Psi_{k,m}(r,\varphi)
\end{aligned} \tag{44}$$

where $\Psi_{k,m}$ is defined in (34) and is known as cylindrical wave function. (44) means that a plane wave can be decomposed into cylindrical waves of exactly the same wavenumber. Conversely,

$$\Psi_{k,m}(r,\varphi) = \int_0^{2\pi} \frac{(-i)^m}{\sqrt{2\pi k}} e^{im\varphi_k} \left(\frac{1}{2\pi}e^{ikr\cos(\varphi-\varphi_k)}\right) d\varphi_k \quad . \tag{45}$$

That is, plane waves of the same wavenumber, with their phases properly shifted according to the direction of the wavevectors, can be superposed to get a cylindrical wave. Alternatively, one says that the (normal) Fourier transform of $\Psi_{k,m}$ is

$$\mathcal{F}(\Psi_{k,m})(k', \varphi_k) = \delta(k-k')\frac{(-i)^m}{\sqrt{2\pi k}} e^{im\varphi_k} \quad . \tag{46}$$

which is nonzero only on a circle of radius k.

Suppose a function $f(r, \varphi)$ is defined on the whole space and its normal Fourier transform is C_{k,φ_k} (C stands for Cartesian. k and φ_k are written as

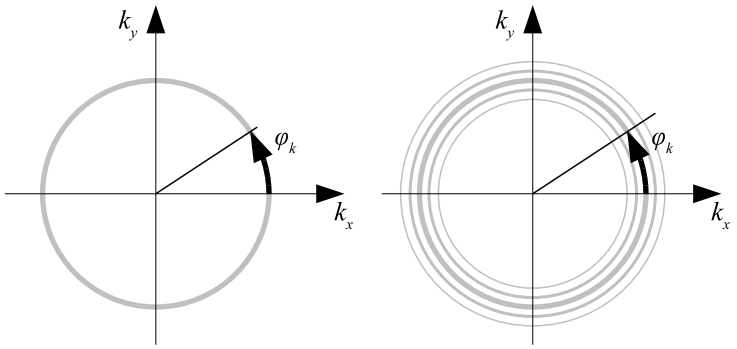

(a) (b)

Figure 4: Illustration of the relation of the polar Fourier coefficients and the normal Fourier coefficients C_{k,φ_k}. (a) When the space is infinite, $P_{k,m}$ is the Fourier coefficient of C_{k,φ_k} with φ_k as the variable. (b) When the space is finite, P_{nm} is the weighted sum of the Fourier coefficients on different circles. With zero boundary condition, the weight function is proportional to (60).

subscripts for consistence of notations here although they take continuous values), it can be expressed as

$$f(r,\varphi) = \int_0^\infty \int_0^{2\pi} C_{k,\varphi_k} \cdot \left(\frac{1}{2\pi} e^{ikr\cos(\varphi-\varphi_k)} \right) k dk d\varphi_k \ . \tag{47}$$

Substituting (44) into (47),

$$f(r,\varphi) = \int_0^\infty \sum_{m=-\infty}^{\infty} \left[\frac{i^m}{\sqrt{k}} \frac{1}{\sqrt{2\pi}} \int_0^{2\pi} C_{k,\varphi_k} e^{-im\varphi_k} d\varphi_k \right] \Psi_{k,m}(r,\varphi) k dk \ . \tag{48}$$

One can recognize immediately that the expression inside the square brackets is just the polar Fourier transform of $f(r,\varphi)$. If it is denoted as $P_{k,m}$, one has

$$P_{k,m} = \frac{i^m}{\sqrt{k}} \frac{1}{\sqrt{2\pi}} \int_0^{2\pi} C_{k,\varphi_k} e^{-im\varphi_k} d\varphi_k \ . \tag{49}$$

The relation is very simple. Except for the factor $(i^m/\sqrt{k})$, $P_{k,m}$ is just the Fourier coefficient of C_{k,φ_k} by considering φ_k as variable. See Figure 4 (a) for an illustration.

(49) can be rewritten as

$$P_{k,m} = \frac{i^m}{k\sqrt{k}} \frac{1}{\sqrt{2\pi}} \int_0^\infty \int_0^{2\pi} \delta(k'-k) e^{-im\varphi_{k'}} C_{k',\varphi_{k'}} k' dk' d\varphi_{k'} \tag{50}$$

for convenience of later discussion.

2.3.2 Transform on Finite Regions

The relation between the polar Fourier transform and the normal Fourier transform is very simple when they are defined on the whole space. Strictly speaking,

it is ambiguous to talk about their relationship when defined on a finite region as the basis functions are defined on regions of different shapes. For convenience of discussion, we consider such a situation here: The normal Fourier transform is defined on a rectangle that is centered at the origin and encloses the disk where the polar Fourier transform is defined. Let the area of the rectangle be A.

We first try to get the expansion of a plane wave in $\{\Psi_{nm}\}$ on the disk. As shown in (44), a plane wave can be expanded in $\Psi_{k,m}$, which in turn can be expanded easily in $\{\Psi_{nm}\}$ on the disk with the help of (28):

$$\begin{aligned} e^{i\mathbf{k}\cdot\mathbf{r}} &= \sum_m i^m J_m(kr) e^{im(\varphi-\varphi_k)} \\ &= \sum_m i^m \sum_n \left[\int_0^a R_{nm}(\rho) J_m(k\rho)\rho d\rho\right] R_{nm}(r) e^{im(\varphi-\varphi_k)} \\ &= \sum_{n,m} i^m \sqrt{2\pi} \left[\int_0^a R_{nm}(\rho) J_m(k\rho)\rho d\rho\right] e^{-im\varphi_k} \Psi_{nm}(r,\varphi) \ . \end{aligned} \quad (51)$$

for $r \le a$. The expression inside the square brackets is the coefficient of $J_m(kr)$ in $R_{nm}(r)$. It can be explicitly expressed by making use of (17). If k_{nm} are selected with the zero boundary condition,

$$\int_0^a R_{nm}(\rho) J_m(k\rho)\rho d\rho = (-1)^n \sqrt{2} k_{nm} \frac{J_m(ka)}{k^2 - k_{nm}^2} \quad (52)$$

and we have

$$e^{i\mathbf{k}\cdot\mathbf{r}} = \sum_{n,m} (-1)^n i^m 2\sqrt{\pi} k_{nm} \frac{J_m(ka)}{k^2 - k_{nm}^2} e^{-im\varphi_k} \Psi_{nm}(r,\varphi) \ . \quad (53)$$

This equation holds for any $\mathbf{k}$, including those appearing in the normal Fourier transform defined on the rectangle, which we denote as $\mathbf{k}_0$.

A function $f(r,\varphi)$ defined on the disk can be extended to the rectangle by padding[1]. Let the normal Fourier coefficients for the padded function be $C_{\mathbf{k}_0}$. On the disk,

$$f(r,\varphi) = \sum_{\mathbf{k}_0} C_{\mathbf{k}_0} \frac{1}{\sqrt{A}} e^{i\mathbf{k}_0\cdot\mathbf{r}} \ . \quad (54)$$

$f(r,\varphi)$ can as well be expanded in $\{\Psi_{nm}\}$,

$$f(r,\varphi) = \sum_{nm} P_{nm} \Psi_{nm}(r,\varphi) \ . \quad (55)$$

With the expansion (53), it is easy to get that

$$P_{nm} = \sum_{\mathbf{k}_0} p(\mathbf{k}_0; n, m)\, C_{\mathbf{k}_0} \quad (56)$$

$$p(\mathbf{k}_0; n, m) = (-1)^n i^m \frac{2\sqrt{\pi}}{\sqrt{A}} k_{nm} \frac{J_m(k_0 a)}{k_0^2 - k_{nm}^2} e^{-im\varphi_{k_0}} \quad (57)$$

[1]It can be proved that the padding scheme does not affect the relations as given in (56) and (61).

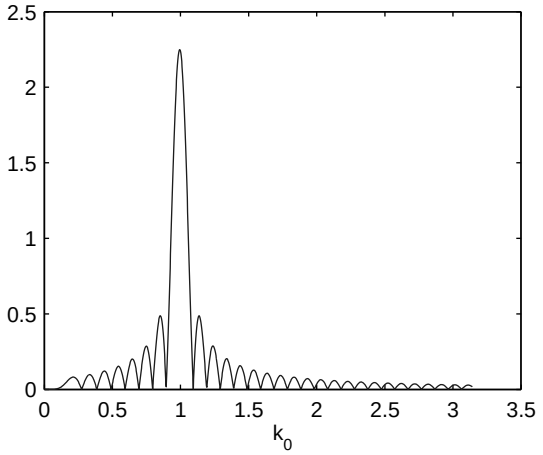

(a) (b)

Figure 5: (a) $\left|\frac{k_0 J_m(k_0 a)}{k_0^2 - k_{nm}^2}\right|$ as a function of k_0 and (b) the real part of $p(\mathbf{k}_0; n, m)$ as defined in (57) for $n = 8$, $m = 5$ and $a = 32$, where $k_{nm} = 0.994$.

for the zero boundary condition. We write the main parts of $P_{k,m}$ and P_{nm} from (50) and (56) for comparison:

$$P_{k,m} \sim \int d\mathbf{k}' \; \delta(k' - k) \; e^{-im\varphi_{k'}} \, C_{k',\varphi_{k'}} \quad , \tag{58}$$

$$P_{nm} \sim \quad \sum_{\mathbf{k}_0} \frac{J_m(k_0 a)}{k_0^2 - k_{nm}^2} e^{-im\varphi_{k_0}} \, C_{\mathbf{k}_0} \quad . \tag{59}$$

When the space becomes finite, the integral over the wave vector is replaced by a summation and the sharp function of the wavenumber $\delta(k' - k)$ is replaced by a more spreading one (see Fig. 4 (b) for an illustration):

$$\frac{J_m(k_0 a)}{k_0^2 - k_{nm}^2} \quad . \tag{60}$$

which has its maximum absolute value at $k_0 = k_{nm}$. According to the asymptotic behavior of Bessel functions, it arrives to its first zeros approximately at $|k_0 - k_{nm}| = \pi/a$ and will oscillatingly decrease on both sides. Fig. 5 (a) shows the absolute value of (60) multiplied by k_0, which comes from the fact that the number of pixels at radius k is approximately proportional to k. Fig. 5 (b) shows the real part of $p(\mathbf{k}_0; n, m)$. One can compare it with the schematic illustration in Fig. 4 (b).

For completeness, if $\{\Psi_{nm}\}$ is determined with the derivative boundary condition, one has

$$P_{nm} = (-1)^n i^m \frac{2\sqrt{\pi}}{\sqrt{A}} \frac{a k_{nm}}{\sqrt{k_{nm}^2 a^2 - m^2}} \sum_{\mathbf{k}_0} \frac{k J_m'(ka)}{k^2 - k_{nm}^2} e^{-im\phi_k} C_{\mathbf{k}_0} \quad . \tag{61}$$

(56) and (61) can be used to calculate the polar Fourier coefficients P_{nm} from the normal Fourier coefficients $C_{\mathbf{k}_0}$, which can be obtained by FFT. This

approach implies sinc interpolation in the spatial domain and is best suited when the underlying original signal is band-limited.

2.4 Comparison with Zernike Polynomials

Basis functions defined with (35) are surely not the only existing orthogonal basis. Actually as $\{R_{nm}|n=1,2,\cdots\}$ for any m forms a basis, one can randomly combine $R_{nm'}$ with $\Phi_m(\varphi)$ and still get an orthogonal basis for functions defined on the disk. But the choice of (35) is the most natural one. It has a clear physical meaning, with the value of k indicating the scale. Apart from the Bessel functions being radial functions, there exists, of course, also an infinity of sets of basis functions on a disk. One of the most famous are Zernike polynomials. Since Teh et al. [11] made a comparison study on different moment methods, which shows that Zernike moments outperform other moment-based methods in terms of overall performance, there are a lot of applications using Zernike moments, e.g. [13–15]. Zernike functions are defined on a unit disk, and, when expressed in polar coordinates, have the following form [3]

$$V_{nm}(r,\varphi) = Z_{nm}(r)e^{im\varphi} \tag{62}$$

where m is any integer, $n \geq 0$ is an integer and is the order of the polynomial, $n \geq |m|$, $n-|m|$ is even. The angular part is the same as that of (35). The radial Zernike function Z_{nm} is a polynomial in r:

$$Z_{nm}(r) = \sum_{s=0}^{\frac{n-|m|}{2}} (-1)^s \frac{(n-s)!}{s!\left(\frac{n+|m|}{2}-s\right)!\left(\frac{n-|m|}{2}-s\right)!} r^{n-2s} \quad . \tag{63}$$

It has $(n-|m|)/2$ zeros between 0 and 1. The orthogonality relation of the radial functions is given by

$$\int_0^1 Z_{nm}(r)Z_{n'm}(r)rdr = \frac{1}{2n+2}\delta_{nn'} \quad . \tag{64}$$

For purpose of comparison, we define the normalized radial function as

$$\widetilde{Z}_{nm} = \sqrt{2n+2}Z_{nm} \quad . \tag{65}$$

The first few normalized radial functions for $m=2$ are shown in Fig. 1 (c). The typical form of $\widetilde{Z}_{nm}$ with relatively large m and n is shown in Fig. 6 together with R_{nm} for comparison. From this figure, one can find that $\widetilde{Z}_{nm}$ has also a wave-like form. Like R_{nm}, it has also a "delay" near the origin for the "wave" to begin; Unlike R_{nm}, the amplitude of the "wave" does not decrease monotonically, instead the "wavelength" decreases with r. As $\{R_{nm}\}$ and $\{\widetilde{Z}_{nm}\}$ are both complete bases, they can be expressed by each other with the help of the following relationship [3]:

$$\int_0^1 Z_{nm}(r)J_m(xr)rdr = (-1)^{\frac{n-m}{2}} \frac{J_{n+1}(x)}{x} \tag{66}$$

where $m \geq 0$ are integers.

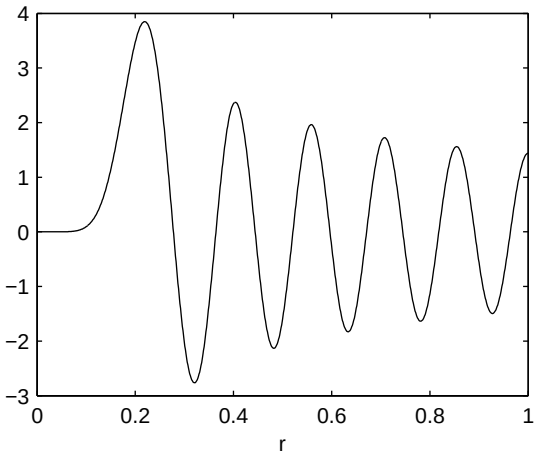

(a)

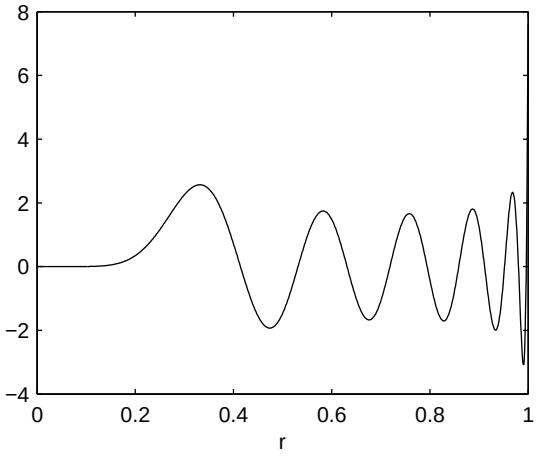

(b)

Figure 6: (a) $R_{(11)8}$ as defined in (27) with derivative boundary condition and (b) $\widetilde{Z}_{(28)8}$ as defined in (65). Both have 10 zeros on $(0, 1)$.

3 Spherical Fourier Tranform

3.1 Basis Functions and Expansion

We will follow the same approach as for polar coordinates, and much of the discussion there also applies here. The expression of the Laplacian in spherical coordinates is given by

$$\nabla^2 = \nabla_r^2 + \frac{1}{r^2}\nabla_\Omega^2 \tag{67}$$

where the radial part is

$$\nabla_r^2 = \frac{1}{r^2}\frac{\partial}{\partial r}\left(r^2\frac{\partial}{\partial r}\right) \tag{68}$$

and the angular part is

$$\nabla_\Omega^2 = \frac{1}{\sin\vartheta}\frac{\partial}{\partial\vartheta}\left(\sin\vartheta\frac{\partial}{\partial\vartheta}\right) + \frac{1}{\sin^2\vartheta}\frac{\partial^2}{\partial\varphi^2} \ . \tag{69}$$

The Helmholtz equation is then given by

$$\nabla_r^2\Psi(r,\vartheta,\varphi) + \frac{1}{r^2}\nabla_\Omega^2\Psi(r,\vartheta,\varphi) + k^2\Psi(r,\vartheta,\varphi) = 0 \ . \tag{70}$$

For a solution of the form $\Psi(r,\vartheta,\varphi) = R(r)\Omega(\vartheta,\varphi)$, one has

$$\Omega(\vartheta,\varphi) = Y_{lm}(\vartheta,\varphi) \tag{71}$$

where Y_{lm} is a spherical harmonic as defined in (5). It satisfies

$$\nabla_\Omega^2 Y_{lm} + l(l+1)Y_{lm} = 0 \ . \tag{72}$$

The corresponding radial part satisfies

$$\frac{1}{r^2}\frac{\partial}{\partial r}\left(r^2\frac{\partial}{\partial r}\right)R + \left(k^2 - \frac{l(l+1)}{r^2}\right)R = 0 \ . \tag{73}$$

Its non-singular solution is

$$R(r) = j_l(kr) \tag{74}$$

where j_l is the so-called spherical Bessel function of order l and is related to the ordinary Bessel Function by

$$j_l(x) = \sqrt{\frac{\pi}{2x}}J_{l+\frac{1}{2}}(x) \ . \tag{75}$$

The spherical Bessel functions satisfy the orthogonality relation

$$\int_0^\infty j_l(k_1r)j_l(k_2r)r^2dr = \frac{\pi}{2k_1^2}\delta(k_1-k_2) \ . \tag{76}$$

Putting the radial part (76) and angular part (71) together, one get the normalized basis function for spherical Fourier transform defined on the whole space

$$\Psi_{k,l,m}(r,\vartheta,\varphi) = \sqrt{\frac{2}{\pi}}kj_l(kr)Y_{lm}(\vartheta,\varphi) \tag{77}$$

When the integral is only over a finite region $[0, a]$, the orthogonality relation generally will not hold, instead

$$\int_0^a j_l(k_1 r) j_l(k_2 r) r^2 dr = \frac{a^2}{k_1^2 - k_2^2} \left[k_2 j_l(k_1 a) j_l'(k_2 a) - k_1 j_l(k_2 a) j_l'(k_1 a) \right] \ . \quad (78)$$

One needs boundary conditions to select a set of orthogonal basis functions. For $r = a$ the S-L boundary condition is

$$R(a) \cos\beta - a^2 R'(a) \sin\beta = 0 \quad (79)$$

with $\beta \in [0, 2\pi)$. With $R(r) = j_l(kr)$, the above boundary condition becomes

$$j_l(ka) \cos\beta - (ka) j_l'(ka) a \sin\beta = 0 \ . \quad (80)$$

Set $x = ka$ and absorb the extra a into the choice of β, the boundary condition becomes

$$j_l(x) \cos\beta - j_l'(x) \sin\beta = 0 \ . \quad (81)$$

If $x_{l1} < x_{l2} < \cdots < x_{ln} < \cdots$ are the nonnegative solutions to (81) with $j_l(x_{ln} r/a)$ nonzero, one can define

$$k_{nl} = \frac{x_{ln}}{a}.$$

The n-th eigenfunction is then $j_l(k_{nl} r)$. The orthogonal relation of the eigenfunctions is

$$\int_0^a j_l(k_{nl} r) j_l(k_{n'l} r) r^2 dr = N_n^{(l)} \delta_{nn'} \ . \quad (82)$$

It can be shown that

$$N_n^{(l)} = \frac{a^3}{2} \left\{ j_l'^2(x_{ln}) + \frac{1}{x_{ln}} j_l(x_{ln}) j_l'(x_{ln}) + \left[1 - \frac{l(l+1)}{x_{ln}^2} \right] j_l^2(x_{ln}) \right\} \ . \quad (83)$$

With the **zero-value boundary condition**, $(x_{l1}, x_{l2}, \cdots, x_{ln}, \cdots)$ are the positive zeros of $j_l(x)$ and

$$N_n^{(l)} = \frac{a^3}{2} j_{l+1}^2(x_{ln}) \ . \quad (84)$$

With the **derivative boundary condition**, $(x_{l1}, x_{l2}, \cdots, x_{ln}, \cdots)$ are the positive zeros of $j_l'(x)$ except for $x_{01} = 0$. And

$$N_n^{(l)} = \frac{a^3}{2} \left[1 - \frac{l(l+1)}{x_{ln}^2} \right] j_l^2(x_{ln}) \quad (85)$$

with the special case

$$N_1^{(0)} = \frac{a^3}{3} \ . \quad (86)$$

The normalized radial basis functions can be defined as

$$R_{nl}(r) = \frac{1}{\sqrt{N_n^{(l)}}} j_l(k_{nl} r) \ . \quad (87)$$

Together with the angular part, the whole basis function for a solid sphere of radius a can be defined as

$$\Psi_{nlm}(r,\vartheta,\varphi) = R_{nl}(r)Y_{lm}(\vartheta,\varphi) \ . \tag{88}$$

A function $f(r,\vartheta,\varphi)$ defined on a $r \leq a$ can be expanded in terms of $\Psi_{nlm}(r,\vartheta,\varphi)$:

$$f(r,\vartheta,\varphi) = \sum_{n=1}^{\infty}\sum_{l=0}^{\infty}\sum_{m=-l}^{l} S_{nlm}\Psi_{nlm}(r,\vartheta,\varphi) \tag{89}$$

where

$$S_{nlm} = \int_0^a \int_0^\pi \int_0^{2\pi} f(r,\vartheta,\varphi)\Psi^*_{nlm}(r,\vartheta,\varphi) r^2 \sin\vartheta dr d\vartheta d\varphi \tag{90}$$

are the spherical Fourier coefficients (S stands for Spherical). For real-valued functions,

$$S_{nlm} = S^*_{nl(-m)} \ . \tag{91}$$

The discussion about mapping an image from Cartesian coordinates to polar coordinates in last section also applies here. The only difference is that for a solid sphere of radius a (in the unit of a voxel size), the "safe" size in spherical coordinates should be $\sqrt{3}a$, $\sqrt{3}\pi a$ and $2\sqrt{3}\pi a$ for r, ϑ and φ respectively.

3.2 Relation to the Normal Fourier Transform in 3D

A plane wave in 3D can be expanded in spherical waves $\Psi_{k,l,m}(r,\vartheta,\varphi)$ as [7]

$$\begin{aligned}\left(\frac{1}{\sqrt{2\pi}}\right)^3 e^{i\mathbf{k}\cdot\mathbf{r}} &= \sqrt{\frac{2}{\pi}}\sum_{l=0}^{\infty}\sum_{m=-l}^{l} i^l j_l(kr)Y_{lm}(\vartheta,\varphi)Y^*_{lm}(\vartheta_k,\varphi_k) \\ &= \frac{1}{k}\sum_{l=0}^{\infty}\sum_{m=-l}^{l} i^l Y^*_{lm}(\vartheta_k,\varphi_k)\Psi_{k,l,m}(r,\vartheta,\varphi) \end{aligned} \tag{92}$$

where $(k,\vartheta_k,\varphi_k)$ are the spherical coordinates of the wave vector $\mathbf{k}$.

Any function $f(r,\vartheta,\varphi)$ defined on the whole space can be expanded in either of the two bases:

$$\begin{aligned} f(r,\vartheta,\varphi) &= \int_0^\infty \int_0^\pi \int_0^{2\pi} C_{k,\vartheta_k,\varphi_k}\left(\frac{1}{\sqrt{2\pi}}\right)^3 e^{i\mathbf{k}\cdot\mathbf{r}}\, k\, \sin\vartheta_k\, dk\, d\vartheta_k\, d\varphi_k \quad (93) \\ &= \sum_{l=0}^{\infty}\sum_{m=-l}^{l}\int_0^\infty S_{k,l,m}\Psi_{k,l,m}(r,\vartheta,\varphi)\, k\, dk \ . \quad (94) \end{aligned}$$

With the relation of the bases as given in (92), one can easily get the relation of the coefficients:

$$S_{k,l,m} = \frac{i^l}{k}\int_0^\pi \int_0^{2\pi} C_{k,\vartheta_k,\varphi_k} Y^*_{lm}(\vartheta_k,\varphi_k)\sin\vartheta_k d\vartheta_k d\varphi_k \ . \tag{95}$$

Except for a constant factor, $S_{k,l,m}$ is the SH coefficient of $C_{k,\vartheta_k,\varphi_k}$ with (ϑ_k,φ_k) as variables.

A function $f(r, \vartheta, \varphi)$ that is defined on a solid sphere of finite radius a can be expanded either in normal Fourier series or in spherical Fourier series. Here the normal Fourier series is defined on a rectangular box which contains the solid sphere and has its center also at the origin. Suppose the volume of the rectangular box is V.

$$\begin{aligned} f(r, \vartheta, \varphi) &= \sum_{\mathbf{k}_0} C_{\mathbf{k}_0} \frac{1}{\sqrt{V}} \, e^{i\mathbf{k}\cdot\mathbf{r}} && (96) \\ &= \sum_{nlm} S_{nlm} \Psi_{nlm}(r, \vartheta, \varphi) \ . && (97) \end{aligned}$$

The Fourier coefficients have the following relationship if k_{nm} are selected with zero boundary condition:

$$S_{nlm} = \left[(-1)^n i^l 4\pi \sqrt{\frac{2a}{V}} \right] \sum_{\mathbf{k}_0} \frac{k_{nl} \, j_l(k_0 a)}{k_0^2 - k_{nm}^2} \, Y_{lm}^*(\vartheta_{k_0}, \varphi_{k_0}) \, C_{\mathbf{k}_0} \ . \tag{98}$$

4 Applications of Polar and Spherical Fourier Transforms

The polar and the spherical Fourier transforms can be regarded as variantions of the Fourier transform. They can have applications in different problems. As the basis function is made up of the radial and the angular part separately, it is easy investigate how the transform coefficients change when the function is rotated.

If a 2D rotation operator $\mathcal{R}(\alpha)$ is defined by

$$\mathcal{R}(\alpha) f(r, \varphi) = f(r, \varphi - \alpha), \tag{99}$$

it works on a basis function of the polar Fourier transform as

$$\begin{aligned} \mathcal{R}(\alpha)\Psi_{nm}(r, \varphi) &= \mathcal{R}(\alpha) R_{nm}(r)\Phi(\varphi) && (100) \\ &= R_{nm}(r) e^{-im\alpha} \Phi(\varphi) && (101) \\ &= e^{-im\alpha} \Psi_{nm}(r, \varphi) \ . && (102) \end{aligned}$$

When it operates on a function $f(r, \varphi)$ with polar Fourier coefficients P_{nm}, the change of the function can be regarded as the change of the coefficients P_{nm}.

$$\begin{aligned} \mathcal{R}(\alpha) f(r, \varphi) &= \mathcal{R}(\alpha) \sum_{n=1}^{\infty} \sum_{m=-\infty}^{\infty} P_{nm} \Psi_{nm}(r, \varphi) && (103) \\ &= \sum_{n=1}^{\infty} \sum_{m=-\infty}^{\infty} P_{nm} \mathcal{R}(\alpha) \Psi_{nm}(r, \varphi) && (104) \\ &= \sum_{n=1}^{\infty} \sum_{m=-\infty}^{\infty} P_{nm} e^{-im\alpha} \Psi_{nm}(r, \varphi) && (105) \end{aligned}$$

With the rotation of $\mathcal{R}(\alpha)$, the coefficient

$$P_{nm} \Longrightarrow P_{nm} e^{-im\alpha}.$$

The phase changes carry the information of rotation, therefore can be used to estimate the rotation. This property can be employed for registration of images.

Under rotation, only the phase of P_{nm} is changed, its magnitude remains the same and is therefore a rotational invariant of the function. It will be called a Polar Fourier Descriptor (PFD). The transform coefficients provide a complete representation of the original function. Theoretically, a complete set of rotational invariant descriptors can be obtained by properly normalizing the coefficients according to the degree of rotational symmetry (similar to the technique in [22]). However, although phase information is very important, there still lacks a systematic and robust way of incorporating this information into the descriptors. By discarding the phases, PFDs are no longer mathematically complete. Nevertheless they still make up a robust set of rotation invariant descriptors.

Rotation in 3D is more complicated than in 2D as there are two angular coordinates now. It is well known that Y_{lm} with $m = -l, -l+1, \cdots, l$ span a subspace that is invariant with respect to the rotation group. When the operator $\mathcal{R}(\alpha, \beta, \gamma)$ (α, β and γ are the Euler angles that represent the rotation) apply to Y_{lm}, one has

$$\mathcal{R}(\alpha, \beta, \gamma) Y_{lm}(\theta, \phi) = \sum_{m'=-l}^{l} D^{(l)}_{m'm}(\alpha, \beta, \gamma) Y_{lm'}(\theta, \phi). \tag{106}$$

where $D^{(l)}_{m'm}(\alpha, \beta, \gamma)$ are the Wigner-D functions. Its exact expression, together with the corresponding definition of the Euler angles, can be found in [4] and will not be given here. As all the variance of the basis function Ψ_{nlm} under rotation is captured by its angular part, one can simply replace Y_{lm} with Ψ_{nlm} in (106) and the equation still holds.

$$\mathcal{R}(\alpha, \beta, \gamma) \Psi_{nlm}(r, \theta, \phi) = \sum_{m'=-l}^{l} D^{(l)}_{m'm}(\alpha, \beta, \gamma) \Psi_{nlm'}(r, \theta, \phi) \ . \tag{107}$$

When a function $f(r, \theta, \varphi)$ with spherical Fourier coefficients S_{nlm} is under rotation $\mathcal{R}(\alpha, \beta, \gamma)$,

$$\mathcal{R}(\alpha, \beta, \gamma) f(r, \theta, \varphi) \tag{108}$$

$$= \mathcal{R}(\alpha, \beta, \gamma) \sum_{n=1}^{\infty} \sum_{l=0}^{\infty} \sum_{m=-l}^{l} S_{nlm} \Psi_{nlm}(r, \theta, \phi) \tag{109}$$

$$= \sum_{n=1}^{\infty} \sum_{l=0}^{\infty} \sum_{m=-l}^{l} S_{nlm} \sum_{m'=-l}^{l} D^{(l)}_{m'm}(\alpha, \beta, \gamma) \Psi_{nlm'}(r, \theta, \phi) \tag{110}$$

$$= \sum_{n=1}^{\infty} \sum_{l=0}^{\infty} \sum_{m=-l}^{l} \left[\sum_{m'=-l}^{l} D^{(l)}_{mm'}(\alpha, \beta, \gamma) S_{nlm'} \right] \Psi_{nlm}(r, \theta, \phi) \tag{111}$$

$D^{(l)}_{m'm}(\alpha, \beta, \gamma)$ with $m, m' = -l, -l+1, \cdots, l$ form a $(2l+1) \times (2l+1)$ matrix

$$\mathbf{D}^{(l)}(\alpha, \beta, \gamma) = \left(D^{(l)}_{m'm}(\alpha, \beta, \gamma) \right) \ ,$$

called the Wigner-D matrix. Define $\mathbf{S}^{(nl)}$ as the column vector made up of S_{nlm} with $m = -l, -l+1, \cdots, l$. With the rotation $\mathcal{R}(\alpha, \beta, \gamma)$,

$$\mathbf{S}^{(nl)} \Longrightarrow \mathbf{D}^{(l)}(\alpha, \beta, \gamma)\mathbf{S}^{(nl)} \quad .$$

The rotation parameters are coded into the change of the spherical Fourier coefficients, and the latter, can be used to estimate the former in turn.

The rotation operator unitary, and its representative matrix $\mathbf{D}^{(l)}(\alpha, \beta, \gamma)$ is then also unitary. It means the magnitude of the vector $\mathbf{S}^{(nl)}$ remains unchanged under rotation. Therefore

$$\|\mathbf{S}^{(nl)}\| = \sqrt{\sum\nolimits_{m=-l}^{l} |S_{nlm}|^2} = \sqrt{\sum\nolimits_{m=-l}^{l} S_{nlm} S_{nlm}^*} \tag{112}$$

is a rotation-invariant property of the object. We call it a Spherical Fourier Descriptor (SFD). A SFD is indexted by two numbers: n and l.

5 Conclusion and Outlook

We propose to use the eigenfunctions of the Laplacian that are separable in polar and spherical coordinates as basis functions for Image analysis. This idea puts the proposed polar and spherical Fourier transform and the normal Fourier transform into the same framework and ensures close resemblance and relation between them.

The changes of the transform coefficients under rotation can be simply expressed as functions of the rotation parameters. This property can be used to estimate rotation angles, which is essential in image registration. We have also shown how rotation-invariant descriptors can be defined on the transform coefficients.

We have discussed how to calculate the coefficients by mapping the data from Cartesian coordinated into polar or spherical coordinates. The angular transforms can be done efficiently with fast programs [23, 24], The radial transform has to be calculated for every coefficient independently. This is surely not an efficient way. Whether fast algorithms exist for radial transforms is a question to be answered.

References

[1] N. N. Lebedev, *Special functions and their applications*, (Translated from Russian by R.A.Silverman) chapter 5, pp. 98-142, Dover, 1972

[2] W. Kaplan, *Advanced Calculus*, pp. 696-698, Addison-Wesley, 1991

[3] M. Born and E. Wolf, *Principles of Optics: Electromagnetic Theory of Propagation, Interference, and Diffraction of Light*, 7th ed. pp. 523-525, Cambridge, 1989

[4] M.Tinkham, *Group Theory and Quantum Mechanics*, pp. 101-115, Dover, 1992

[5] Wikipedia, "Sturm-Liouville theory," `http://en.wikipedia.org/wiki/Sturm-Liouville_theory`

[6] Weisstein, Eric W, "Jacobi-Anger Expansion." From MathWorld–A Wolfram Web Resource. http://mathworld.wolfram.com/Jacobi-AngerExpansion.html

[7] K.E. Schmidt, "The expansion of a plane wave", http://fermi.la.asu.edu/PHY577/notes/plane.pdf

[8] S. Erturk, T.J. Dennis, "3D model representation using spherical harmonics," *Electronics Letters*, vol. 33, no.11, pp.951-952, 22 May 1997

[9] M. Kazhdan, T. Funkhouser and S. Rusinkiewicz, "Rotation Invariant Spherical Harmonic Representation of 3D Shape Descriptors," *Symposium on Geometry Processing*, pp. 167-175, June 2003

[10] H. Huang, L. Shen, R. Zhang, F. Makedon, A. Saykin, and J. Pearlman, "A Novel Surface Registration Algorithm in Medical Modeling Applications," *IEEE Trans. on Information Technology in Biomedicine*, vol. 11, no. 4, pp. 474-482, 2007

[11] C.-H. Teh and R.T. Chin, "On image analysis by the methods of moments," *IEEE Trans. Pattern Analysis and Machine Intelligence*, vol. 10, no. 4, pp. 496-513, 1988

[12] Y. Zana and R.M. Cesar-Jr."Face recognition based on polar frequency features," *ACM Trans. Applied Perception*, vol. 3, no. 1, pp. 62-82, 2006

[13] A. Khotanzad and Y. H. Hong, "Invariant Image Recognition by Zernike Moments," *IEEE Trans. Pattern Analysis and Machine Intelligence*, vol. 12, no. 5, pp. 489-497, May 1990

[14] W.-Y. Kim and Y.-S. Kim, "Robust Rotation Angle Estimator," *IEEE Transactions on Pattern Analysis and Machine Intelligence* , vol. 21, no. 8, pp. 768-773, 1999

[15] E.M. Arvacheh and H.R. Tizhoosh, "Pattern Analysis Using Zernike Moments," *Instrumentation and Measurement Technology Conference, 2005. IMTC 2005. Proceedings of the IEEE* Volume 2, pp. 1574-1578, 16-19 May 2005

[16] A. Averbuch, R.R. Coifman, D.L. Donoho, M. Elad, M. Israeli,"Accurate and Fast Discrete Polar Fourier Transform," : Signals, Systems and Computers, 2003. Conference Record of the Thirty-Seventh Asilomar Conference on, vol. 2, pp. 1933-1937, 2003

[17] A. Makadia, L. Sorgi and k. Daniilidis, Rotation estimation from spherical images, "Rotation estimation from spherical images," *Pattern Recognition, ICPR 2004, Proceedings of the 17th International Conference on*, vol. 3, pp. 590-593, 23-26 Aug. 2004

[18] R. Skomski, J.P. Liu, and D.J. Sellmyer, "Quasicoherent nucleation mode in two-phase nanomagnets," *Phys. Rev. B* 60, pp. 7359-7365, 1999

[19] B. Pons, "Ability of monocentric close-coupling expansions to describe ionization in atomic collisions" *Phys. Rev. A* 63, pp. 012704, 2000

[20] R. Bisseling and R. Kosloff "The fast Hankel transform as a tool in the solution of the time dependent Schringer equation," *Journal of Computational Physics*, vol. 59, no. 1, pp. 136-151, May 1985

[21] D. Lemoine, "The discrete Bessel transform algorithm," *J. Chem. Phys.* 101, pp. 3936-3944, 1994

[22] H. Burkhardt, *Transformationen zur lageinvarianten Merkmalgewinnung*, Ersch. als Fortschrittbericht (Reihe 10, Nr. 7) der VDI-Zeitschriften, VDI-Verlag, 1979

[23] FFTW Home Page, `http://www.fftw.org/`

[24] Fast Spherical Harmonic Transforms, `http://www.cs.dartmouth.edu/~geelong/sphere/`